Elsevier Editorial System(tm) for Molecular and Cellular Endocrinology
Manuscript Draft

Manuscript Number: MCE-D-14-00306R1

Title: Identification of transmembrane domains that regulate spatial arrangements and activity of prokineticin receptor 2 dimers

Article Type: Research Paper

Keywords: G-protein coupled receptor (GPCR); Prokineticin receptor 2 (PKR2); dimerization; signaling; bioluminescence resonance energy transfer (BRET); molecular modeling.

Corresponding Author: Dr. Aylin Hanyaloglu,

Corresponding Author's Institution: Imperial College London

First Author: Silvia Sposini, BSc, MSc

Order of Authors: Silvia Sposini, BSc, MSc; Gianluigi Caltabiano, PhD; Rossella Miele, ph.D; Aylin C Hanyaloglu, PhD

Abstract: The chemokine prokineticin 2 (PK2) activates its cognate G protein-coupled receptor (GPCR) PKR2 to elicit various downstream signaling pathways involved in diverse biological processes. Many GPCRs undergo dimerization that can modulate a number of functions including membrane delivery and signal transduction. The aim of this study was to elucidate the interface of PKR2 protomers within dimers by analyzing the ability of PKR2 transmembrane (TM) deletion mutants to associate with wild type (WT) PKR2 in yeast using co-immunoprecipitation and mammalian cells using bioluminescence resonance energy transfer. Deletion of TMs 5-7 resulted in a lack of detectable association with WT PKR2, but could associate with a truncated mutant lacking TMs 6-7 (TM1-5). Interestingly, TM1-5 modulated the distance, or organization, between protomers and positively regulated Gαs signaling and surface expression of WT PKR2. We propose that PKR2 protomers form Type II dimers involving TMs 4 and 5, with a role for TM5 in modulation of PKR2 function.

Imperial College London

Department of Surgery and Cancer
Imperial College London

Institute of Reproductive and Developmental Biology (IRDB)
Hammersmith Hospital Campus
Du Cane Road
London
W12 0NN

Tel:+44 (0) 207 594 2128 Fax: +44 (0) 207 594 2184

a.hanyaloglu@imperial.ac.uk
www.imperial.ac.uk
www1.imperial.ac.uk/medicine/about/institutes/irdb

Aylin Hanyaloglu PhD
Lecturer

10th October 2014

Prof. Carolyn Klinge
Editor
Molecular and Cellular Endocrinology

Dear Professor Klinge,

Thank you for the review of our manuscript, entitled; “Identification of transmembrane domains that regulate spatial arrangements and activity of prokineticin receptor 2 dimers” by; S. Sposini, G. Caltabiano, A. Hanyaloglu and R. Miele (manuscript ref. no. MCE-D-14-00306).

We have carefully considered the reviewers' comments and suggestions and extensively edited the manuscript to address them, including addition of new data. In particular, we have included further controls to confirm that BRET-tagged receptors are functional and inclusion of BRET analysis in both HEK and CHO cells. We have also made improvements to the text in order to ensure a clearer understanding of the methodology and results. We now believe that we have fully addressed all of the concerns raised by the Reviewers and, therefore, wish to submit the revised manuscript for your consideration.

Specific responses to comments together with descriptions of new data added and changes made in the text and figures, are detailed in the attached "Response to Reviewers." We believe that the revised manuscript is substantially improved, and we thank the reviewers for their positive comments and for aiding with refinement and clarity of this study.

Thank you again for your consideration, and we hope that you will now find our work acceptable for publication.

Yours sincerely,

Aylin Hanyaloglu and Rosella Miele

Response to Reviewers

Reviewer #1:
There is one concern: the backgrounds of the images in figure 2 are different-- which suggests either differential processing or alteration of the contrast.

We would like to thank the reviewer for their overall positive comments. In regards to Figure 2 we would like to assure the reviewer there was no post-acquisition modification of the figures. The development of film in the laboratory in Rome is carried out without an automated film processor but incubation in individual baths of developer, which can result in background differences of the films. The original films were presented as photographed images in the original submission thus we have now scanned the original films and presented them in grey-scale to improve image clarity (please see new Figure 2) but again we would like to emphasize that no alterations of the contrast were made. We hope that the reviewer now finds these images clearer and more importantly does not change our conclusions that WT PKR2 can associate with PKR2 lacking TMs 6 and/or 7, but not with the PKR2 truncation mutant lacking TMs 5-7 (TM1-4).

Reviewer #2:

Page 1, Abbreviations. CHO is written twice. The authors sometimes write transmembrane, sometimes use the abbreviation TM.

We thank the reviewer for identifying these corrections. These have now been altered. Please see Abbreviations bottom of p.3. Plus transmembrane is now only used for the first time it is mentioned in the Introduction, p3, line 1 (excluding the abstract).

Page 3, Introduction. References need to be added to the last phrase, which also need to be reviewed. G<alpha>q also activates the stimulation of the mitogen-activated protein kinase.

We have now modified this paragraph (please see p.3, paragraph 2, lines 7-12) to be clearer that although Gq signaling is the classic PKR2 pathway, this receptor can couple to other G proteins. In regards to MAP kinase signaling, the only report of which G proteins are involved in this pathway in the literature are studies carried out in the presence of the Gi inhibitor Pertussis Toxin (Lin R et al, 2002, PMID 11751915) that demonstrated complete block of MAPK signaling in this study. We are not aware of any report of pertussis-toxin independent MAPK signalling by PKR2, or where Gq/11 inhibitors or siRNA studies have been carried out. It is certainly possible that other G proteins, or non-G protein-dependent pathways could be involved in PKR2-mediated MAPK signaling in other cell types but this has not been directly demonstrated.

Page 4, Third paragraph. First line should read GPCRs.

We have altered paragraph 4, line 1 (p.4) that starts 'Despite the recognized importance of GPCR dimerization in receptor function….'. to: 'Despite the recognized importance of dimerization in receptor function..'

Page 5, Material and Methods, Vector Construction section. Where did you get the human PKR2? It would be helpful to explain here that N term-R2-HIS is deleted for the region 1-18. Where is the tag in the HA-tagged PKR2? I assume it is N-terminal but it is helpful to add this information. It would be better to be more explicit about the receptor deletions. The authors write TM1-5, TM1-6, etc. They

should also add where in the nucleotide sequence and in the amino acid sequence the deletion was made and the size of the deleted receptor (amino acids number).

We have now added further information on how PKR2 was obtained, the nature of the His-tagged receptor, that the HA-tagged receptor is indeed N-terminal (see also modified Fig. 1) and the amino acid residues that were mutated to stop codons for the TM deletion mutants. Please see Materials and Methods, Section 2.1, p.5.

Page 7, Bioluminescence resonance energy transfer (BRET). The authors should add which cells were transfected in this experiment.

We have now added that both HEK 293 and CHO cells were transfected for BRET studies (see Section 2.6, p.8, paragraph 2, line 1) as we have also included additional BRET data carried out in CHO cells (see related comment below).

The authors did not describe the immunoprecipitation procedure in the Methods section. The amount of receptors transfected should be added to the methods, the authors added this information to the BRET studies but not to other procedures.

We apologize to the reviewer that this information was not included in the original submission. We have now added extra information on the IP procedure used. Please see Section 2.4, p7, paragraph 3. We have also added the amount of receptors transfected for all the signalling and flow cytometry assays (please see section 2.7, 2.8 and 2.9, p8-9.

Page 9, Results. It would be better to be consistent in the description of the mutants.

We have now ensured that description of the mutants in the Results (see p.10, section 3.1, paragraph 2, lines 5-9) is consistent throughout the manuscript.

Page 9, Results, Second paragraph. It would be helpful to add the expected molecular weight for PKR2 monomers and dimers. "....as evidenced by the bands with molecular weight corresponding to the sum of the WT and deleted receptor types."

We have added the predicted molecular weights of individual monomers of WT and mutant receptors plus combined sizes of the WT and deletion mutant dimers. Please see Results p.10, paragraph 2, lines 7-9 and paragraph 3 lines 7-8.

Figure 1. I don't understand why the TM1-4 is not included in the figure (it is in the supplemental figure). Please explain what CyCp is. A good control to show specificity of HIS beads would be to use yeast membranes transformed only with PKR2WT showing no bands in the western blot.

We agree that the TM1-4 should be in the main Figure 2 and have now moved this data from supplemental Figure 1 to Figure 2 (now Fig. 2D).

The control suggested by the reviewer was not used in this study as it was previously employed in our prior published work demonstrating PKR2 dimerization in yeast (Marsango et al, 2011 PMID: 21161321).

Reference to CyCp was an error, which we apologise for, and should be Cy12946, the yeast strain that was employed in these studies (details described in Materials and Methods, Section 2.2, p.6, paragraph 5).

Page 10, Results. The authors claim that they assessed if Rluc8 and Venus tags alter the receptor function testing the activation of cAMP signaling pathway. However, they did not assess receptor activation via G<alpha>q, which is a well-established PKR2 signaling pathway and could be affected by the tags.

The reviewer makes a valid comment given the broad G protein-coupling ability of PKR2. We have now included additional data testing the ability of the BRET-tagged receptors to increase intracellular calcium levels using a calcium indicator dye Fluo4-AM and confocal imaging. As observed with Cre-Luc responses (Fig. 3A), there were no significant differences in the ability of the BRET-tagged receptors to increase intracellular calcium levels following treatment with the ligand Bv8, compared to untagged PKR2 (please see new Fig. 3B). Thus confirming that, as for many GPCRs, C-terminal addition of the BRET tags does not impact PKR2 activity (please see Results section, p.11, paragraph 2).

Page 10, Homodimerization of PKR2 in mammalian cells via BRET. The authors should write, "HEK293 cells were co-transfected…." Throughout the manuscript the authors should always add the cell type used and not just write cells.

We have now ensured that the cell type is stated for all experiments described in the Results and in the Figure Legends. Please see Results p.11, Section 3.3, paragraph 3, line 1 as an example.

Page 12, Results. The authors state that HEK293 cells have an endogenous response to PKR2 ligand Bv8 implying that these cells express PKR2 (or PKR1) but the data is not shown. It would be informative to add these data because several groups published papers with PKR2 in vitro studies using HEK293 cells. If the authors consider that HEK293 cells express PKR2 it would be better to perform the BRET studies in CHO cells. Is there a reason for not doing that? The authors then compare BRET measurements in CHO and HEK293 cells but in Figure 3 of the supplement they just show the graph from CHO cells and don't have the measurements with the comparisons between the two cell lines.

We have now included this data to the supplementary figures (Suppl Fig.2). Here we observed that treatment of untransfected HEK 293 cells with Bv8 resulted in an increase in phospho-ERK levels following 5 min of ligand stimulation. Furthermore, this is consistent with prior reports observing similar endogenous responses to Bv8 in HEK 293 cells (Lin et al, 2002, PMID 11886876) and that PKR2, but not PKR1, is detected via microarray analysis for the GPCR superfamily members in HEK 293 cells (Atwood et al, 2011 PMID:21214938). Because of this observation we decided to perform our signaling studies in CHO cells following confirmation that Bv8 did not induce Cre-Luc responses in cells not transfected with PKR2 (now included in modified Fig.7 A). We have also conducted additional BRET data (Suppl. Fig 3) to demonstrate that the BRET profiles observed in HEK cells are similar to that in CHO cells. Importantly we observe that the BRET signals in CHO cells between WT and TM1-5 are greater that WT-WT or WT-TM1-6 and that no BRET signals were observed between WT and TM1-4, as we observed for HEK 293 cells (Fig. 5). The presence of PKR2 in HEK cells are most likely at a far lower level than the overexpression BRET experiments with untagged PKR2, to impact on BRET signal profiles. We have not put direct comparisons in the same figure of the two cell lines as the BRET saturation curves are all in Figure 5 and we believe the similarities are clear, without having to show the BRET saturation curves again for the HEK 293 cells in the supplementary Figure.

Page 12, Lack of TM6-7 positively regulates WT PKR2 signaling and expression. The authors state "In contrast, no agonist induced signaling was observed in cells expressing TM1-4 or TM1-5 alone. " As the authors mention in the abstract "The chemokine prokineticin 2 (PK2) activates its cognate G protein-coupled receptor (PKR2) to elicit various downstream signaling pathways…" They are assessing G<alpha>s signaling pathway, which should the emphasized. Biased signaling through G-protein-coupled PKR2 receptors harboring missense mutations has been described and one cannot rule out biased signaling with deletions of the receptor.

The reviewer raises a valid and interesting point. We have now explicitly stated that we are assessing Gs signaling pathways, e.g. please see Abstract, line 9. Because of this we have also raised the question in the Discussion of whether the impact of TM1-5 on WT PKR2 signaling could be extended to the diverse signaling pathways activated by PKR2, or whether this specifically effects Gs signaling only (please See Discussion, p.16, paragraph 2, lines 3-5.

In the Discussion the authors should discuss more about the clinical implications of their findings. Numerous heterozygous PKR2 variants have been identified in patients with Kallmann syndrome and isolated hypogonadotropic hypogonadism and several of them do not segregate in families. It has been shown that a PKR2 heterozygous mutation exerts a dominant negative effect on WT PKR2. It may be possible that some PKR2 variants can result in a "dominant positive" effect (or rescue of the receptor) and therefore don't segregate in the families because they are not the cause of the phenotype. This is the first description of a mutant PKR2 exerting a positive effect on WT PKR2 and even though this study did not assess point mutations it could help to elucidate why so many heterozygous PKR2 variants do not segregate in families.

We agree that this is an interesting point to add to the Discussion. Please see addition of a new paragraph on the clinical implications in relation to Kallman Syndrome and the impact of a dominant positive effect of a mutant in such a condition (p.16, paragraph 2).

Figure 3 legend, last phrase an "e" is missing in the word presented.

This has now been corrected. Please see p.23, Fig. 3 legend, line 4.

Figure 7 legend is incorrectly describing that TM1-5-Venus was transfected but it should read TM1-5.

For these experiments described in Figure 7 we used TM1-5-Venus to enable us to identify populations that were specifically co-expressing HA-tagged WT PKR2 and TM1-5-Venus via flow cytometry in order to determine effects of TM1-5 on WT PKR2 expression.

Figure 8 legend should define what is in yellow and green in C. To be consistent define what is Type II dimers in the legend the same way Type I was defined.

Please see modified Figure 8 legend (p.25).

Identification of transmembrane domains that regulate spatial arrangements and activity of prokineticin receptor 2 dimers

Sposini S[1,2], Caltabiano G[3], Hanyaloglu AC[2*], Miele R[1]

1, Dept. Biochemical Science, Sapienza Università di Roma, Italy

2, Institute of Reproductive and Developmental Biology, Dept. Surgery and Cancer, Imperial College London, UK

3, Laboratori de Medicina Computacional, Unitat de Bioestadística, Facultat de Medicina, Universitat Autònoma de Barcelona, Spain

*To whom correspondence should be addressed:

Aylin C. Hanyaloglu; Institute of Reproductive and Developmental Biology, Dept. Surgery and Cancer, Imperial College London, Hammersmith Campus, Du Cane Road, London, W12 0NN, UK

Tel: +44 (0)20 759 42128; Fax: +44 (0)20 759 42148; Email: a.hanyaloglu@imperial.ac.uk

Abstract:

The chemokine prokineticin 2 (PK2) activates its cognate G protein-coupled receptor (GPCR) PKR2 to elicit various downstream signaling pathways involved in diverse biological processes. Many GPCRs undergo dimerization that can modulate a number of functions including membrane delivery and signal transduction. The aim of this study was to elucidate the interface of PKR2 protomers within dimers by analyzing the ability of PKR2 transmembrane (TM) deletion mutants to associate with wild type (WT) PKR2 in yeast using co-immunoprecipitation and mammalian cells using bioluminescence resonance energy transfer. Deletion of TMs 5-7 resulted in a lack of detectable association with WT PKR2, but could associate with a truncated mutant lacking TMs 6-7 (TM1-5). Interestingly, TM1-5 modulated the distance, or organization, between protomers and positively regulated $G_{\alpha s}$ signaling and surface expression of WT PKR2. We propose that PKR2 protomers form Type II dimers involving TMs 4 and 5, with a role for TM5 in modulation of PKR2 function.

Keywords: G-protein coupled receptor (GPCR), Prokineticin receptor 2 (PKR2), dimerization, signaling, bioluminescence resonance energy transfer (BRET), molecular modeling.

1. Introduction

G-protein-coupled receptors (GPCRs) [4] comprise the largest family of transmembrane (TM) receptors in the human genome, responding to a plethora of signals that activate second messenger signaling cascade mechanisms via heterotrimeric G-proteins. Their diversity means they impact nearly every aspect of human physiology and pathophysiology and represent the most successfully exploited drug targets, due to their central role in pathogenesis of human disease. The linear model of G protein signaling cannot explain the diversity in GPCR function *in vivo*. This has driven our current understanding in the complex mechanisms that this superfamily of receptors can employ. One key mechanism is the ability of GPCRs to exist as dimers and/or higher order oligomers (Palczewski, 2010) which can both diversify and define receptor function including modulation of agonist and antagonist affinity, membrane trafficking and signal transduction specificity (Rivero-Müller et al., 2013).

The mammalian prokineticin family are involved in diverse biological processes, including neurogenesis, angiogenesis, carcinogenesis, circadian rhythm regulation, inflammation, immune system modulation, pain perception and GnRH ontogeny (Cheng et al., 2002; Giannini et al., 2009; LeCouter et al., 2001; Ng et al., 2005; Shojaei et al., 2007). Their importance in these pathways are underscored by the identification of mutations in prokineticin 2 (PK2) and prokineticin receptor 2 (PKR2) in patients affected with Kallmann syndrome (KS) and/or idiopathic hypogonadotropic hypogonadism, disorders characterized by delayed puberty and infertility (Cole et al., 2008; Dodé et al., 2006; Pitteloud et al., 2007). Binding of PK2 to its cognate GPCR, PKR2, is well known to activate $G\alpha_{q/11}$ signaling leading to the accumulation of inositol phosphate and the mobilization of intracellular Ca^{2+} (Lin D.C., 2002; Ngan and Tam, 2008). However, PKR2 can also activate other heterotrimeric G protein pathways including inhibition of cAMP accumulation through $G\alpha_{i/o}$ proteins, which in certain cell types also mediates mitogen-activated protein kinase signaling (Lin R. et al., 2002), or even elevation of intracellular cAMP levels via $G\alpha_{s}$ (Chen et al.,2005).

[4]Abbreviations: BRET, Bioluminescence Resonance Energy Transfer; CHO, Chinese hamster ovary; Cre-Luc, cyclic AMP response element-luciferase; GPCRs, G protein-coupled receptors; HEK, Human embryonic kidney; KS, Kallmann Syndrome; PK2 prokineticin 2; PKR2, prokineticin receptor 2; Rluc, *Renilla* luciferase; TM, transmembrane; WT, wild-type.

We have previously demonstrated that PKR2 undergoes dimerization using the baker's yeast *Saccharomyces cerevisiae,* an accepted experimental system for characterizing human receptor pharmacology and signal transduction mechanisms (Dowell and Brown, 2002; Marsango et al., 2011). Dimerization of PKR2 was sufficient for full receptor activity as co-expression of signal and binding deficient receptors was able to rescue PKR2 signaling via functional complementation. Importantly, we have demonstrated that endogenous PKR2 forms dimers in neutrophils, suggesting it is a relevant form of receptor activity *in vivo* (Marsango et al., 2011).

Despite the recognized importance of dimerization in receptor function, identifying which interfaces are involved and how an individual dimer is formed remains an unanswered question. Numerous molecular, biochemical and biophysical studies, including recent crystallography studies, suggest different TM segments are implicated in this process, depending on the specific receptor under investigation (Huang et al., 2013; Manglik et al., 2012; Palczewski, 2010; Wu et al., 2010; Zhu et al., 2013).

Therefore the aim of this study was to elucidate the dimer interface formed by PKR2 and thereby the organization of PKR2 monomers in the complex. Utilizing PKR2 deletion mutants in yeast and in mammalian cells, via both biochemical and biophysical approaches, we identify that PKR2 dimers form an interface with a prominent role for TM5 in modulating dimer organization. Importantly, we demonstrate that TM5 may play an unprecedented role in regulating receptor activity.

2. Materials and methods

2.1 PKR2 constructs

The human PKR2 was used as a PCR template for all PKR2 constructs. Human PKR2 cDNA was amplified by PCR using as template human brain Marathon-Ready cDNA (Clontech) using the available PKR2 sequence (accession n. AL121755). The PKR2 mutants used in this study are illustrated in Figure 1 and oligonucleotides used for construction of the various mutants in Table 1. ΔNter-PKR2-HIS has the first 18 N-terminal aminoacids of PKR2 sequence deleted and contains 6xHIS residues at its C-terminal tail. TM1-6, TM1-5 and TM1-4 contain a stop codon after amino acid 311, 235 and 211 of the PKR2 sequence; the mutations are L312X, V236X and W212X, respectively.

Yeast constructs:

The procedure to construct WT PKR2 pGAD, TM1-6 pGAD, TM1-5 pGAD and ΔN term-R2-HIS pYES3/CT has been previously described (Marsango et al., 2011). To construct mutant TM1-4 that contains a stop codon in position 212, PCR was performed with oligonucleotides R2 BamHI up and TM1-4 dw, the product digested and ligated into p426.

Mammalian cell constructs:

- PKR2 WT

HA-PKR2— PKR2 was inserted into pCMV using KpnI and NotI restriction sites downstream and in-frame with a region encoding the metabotropic glutamate receptor 5 signal sequence followed by a haemagglutinin (HA) tag.

PKR2-Venus—The primers were as follows: R2 HindIII up; R2 SalI dw. The amplified fragment was digested and ligated into pCMV4 upstream and in-frame with Venus ligated between SalI and XhoI. Venus YFP cDNA was kindly provided by Atsushi Miyawaki (RIKEN Brain Science Institute).

PKR2-Rluc8—The primers were as follows: R2 BamHI up; R2 SalI dw. The amplified fragment was digested with BamHI and SalI and ligated into pCMV2 upstream and in-frame with *Renilla* luciferase 8 (Rluc8) cloned XhoI-ApaI. Rluc8 cDNA was kindly provided by Sanjiv Gambhir (Stanford University).

- PKR2 mutants

TM1-6-Rluc8—The primers were as follows: R2 BamHI up; TM1-6 dw, that introduces a hydrophobic linker sequence to ensure Rluc8 is cytoplasmic. The amplified fragment was digested with BamHI and XhoI and ligated into pCMV2 upstream and in-frame with Rluc8 cloned XhoI-ApaI.

TM1-5-Venus—The primers were as follows: R2 HindIII up; R2 TM1-5 dw. The amplified fragment was digested and ligated into pCMV4 upstream and in-frame with Venus ligated between SalI and XhoI.

TM1-4-Rluc8—The primers were as follows: R2 BamHI up; TM1-4 dw, that introduces a hydrophobic linker sequence to ensure Rluc8 is cytoplasmic. The amplified fragment was digested with BamHI and SalI and ligated into pCMV2 upstream and in-frame with Rluc8 cloned XhoI-ApaI.

2.2 Yeast culture and transformation

The *Saccharomyces cerevisiae* strain used for PKR2 expression was Cy12946 (MATa FUS1p-HIS3 GPA1Ga i2(5) can1 far1D1442 his3 leu2 sst2D2 ste14::trp1::LYS2 ste3D1156 tbt1-1 trp1 ura3), a generous gift from Addison D. Ault (Princeton University, USA). Specifically, Cy12946 expresses a chimeric Gα subunit (GPA1Gαi2(5)) in which the carboxyl terminal five amino acids of the yeast Gα subunit, GPA1, are replaced by the carboxyl-terminal five residues of mammalian Gαi2. The use of GPA1 Gαi2(5) required deletion of SST2, which down-regulates the pheromone response pathway by accelerating the GTPase activity of GPA1.

Transformation of Cy12946 yeast cells was performed by the lithium acetate protocol (Ausubel et al., 1994). The yeast strain Cy12946 was co-transformed with ΔN term-R2-HIS and either WT, TM1-6, TM1-5 or TM1-4, generating four different strains that stably and equally co-express ΔN term-R2-HIS in combination with each of the mutants. Yeast transformants were grown at 30ºC to mid-logarithmic phase in appropriate

selection media containing 2% raffinose as the sole carbon source. Protein expression was induced by the addition of galactose to a final concentration of 20 g/l.

2.3 Total yeast membranes

Yeast cells from a 200 ml overnight culture (OD_{600} 0.8-1) were collected by centrifugation. All subsequent manipulations were conducted on ice. Cells were washed in water and re-centrifuged. The cell pellet was then weighed and resuspended in ice-cold lysis buffer (25 mM Tris-HCl pH 7.4, 150 mM NaCl, 1 mM PMSF and 10 μg/ml leupeptin and pepstatin). Glass beads were added to the suspension, and the cells were broken by vigorous vortexing. To minimize protein denaturation, the sample was put on ice for 1 min after vortexing. This procedure was repeated four times. Samples were centrifuged at 13,200 rpm for 1 min. Subsequently, membranes were pelleted by centrifugation at 40,000×g for 40 min. The resulting membrane pellet was resuspended in lysis buffer with addition of 1% Triton X-100 and incubated for 1 h at room temperature. Samples were centrifuged at 40,000×g for 30 min and the supernatant containing the membrane extracts, were stored at -80°C.

2.4 Immunoprecipitation and Western blotting of yeast membrane extracts

Samples were immunoprecipitated by metal chelation chromatography using a Ni-NTA His•Bind resin following the batch purification under native conditions according to manufacturer's instructions (Novagen). Eluates were fractionated by SDS–PAGE on a 10% gel and transferred to a polyvinylidene difluoride membrane. The membrane was probed with anti-His monoclonal antibody horseradish peroxidase conjugate (Roche) 1:5000, or with anti-PKR2 goat polyclonal antibody (sc-54316, Santa Cruz Biotechnology) 1:3000 followed by rabbit anti-goat IgG horseradish peroxidase conjugate. The immunoreactive bands were visualized using an ECL detection system (BM Chemiluminescence Blotting Substrate, Roche).

2.5 Mammalian cell culture and transfections

Human embryonic kidney (HEK) 293 cells and Chinese hamster ovary (CHO) cells (American Type Culture Collection) were maintained in DMEM or MEM, respectively, containing 10% FBS and

penicillin/streptomycin (100 U/ml) at 37°C in 5% CO2. Transient transfections of HEK 293 cells were performed with Lipofectamine 2000 (Invitrogen) according to the manufacturer's instruction and cells were assayed 72 h post-transfection. CHO cells were transiently transfected with JetPEI (Polyplus) and assayed 48 h post-transfection.

2.6 Bioluminescence resonance energy transfer (BRET)

HEK 293 and CHO cells were transiently transfected with constant amounts of receptor-Rluc8 (0.5 μg) and increasing amounts of receptor-Venus (0-3.5 μg) and assayed 72 h (HEK 293) or 48 h (CHO) post-transfection. On the day of the assay, cells were washed and harvested in PBS and seeded at a density of approximately 200,000 cells/well into white flat bottom 96-well plates. The Rluc substrate Coelentrazine H (Promega) was added at a final concentration of 5 μM, and BRET values emitted at 475nm/535nm for a total of 10 cycles. In parallel cells, fluorescence of the Venus-tagged receptor was determined at 485nm ex/540nm em. All the readings were taken using a luminescence plate reader (LUMIstarOPTIMA, BMG Labtech). The BRET ratio was calculated by dividing the signal at 535nm over that emitted by 475nm, and net BRET values calculated by subtracting from all readings the basal BRET ratio obtained when receptor-Rluc8 was expressed alone. Net BRET values were plotted as a function of Venus⁻$Venus_0$/Rluc8 values. Data were fitted using a nonlinear regression equation (GradPad Prism V5). All experiments were conducted in duplicate and at least three times.

2.7 Flow cytometry

Flow cytometry was used to quantitate cell surface HA-WT in presence and absence of TM1-5-Venus. CHO cells transiently transfected with either HA-WT (1.5 μg) or HA-tagged PKR2 (1.5 μg) with TM1-5-Venus (1.5 μg) were fed with mouse anti-HA antibody (Covance) for 20 min at 37 ºC. Cells were washed and collected PBS supplemented with 2% FBS and incubated with Alexa fluor 647 anti-mouse antibody (Invitrogen) for 60 min at 4 ºC. Cells were washed with PBS / 2% FBS and the fluorescence intensity of 10,000 cells was collected for each sample using a FACSCalibur flow cytometer (BD Biosciences). Duplicate readings were taken, and at least 3 independent experiments carried out.

2.8 cAMP responsive element - luciferase reporter gene assay

The cAMP responsive element-luciferase (Cre-Luc) reporter construct was kindly provided by Ilpo Huhtaniemi (Imperial College London, UK). CHO cells were transiently transfected with receptors (1.5 μg) and constant amounts of Cre-Luc (0.5 μg) with *Renilla* luciferase (0.05 μg) as a normalization control. 48 h after transfection cells were stimulated with Bv8 100 nM (Miele et al., 2010) for 5 h. Cre-Luc activity was measured using the Steady Lite Plus (Perkin Elmer) according to the manufacturer's protocol and samples read on a luminescence plate reader (LUMIstarOPTIMA, BMG Labtech). All experiments were conducted in quadruplicate and at least four times.

2.9 Calcium assay

CHO cells were transiently transfected with receptors (1.5 μg) and assayed 48 h after transfection. The assay was performed using Fluo-4 Direct™ Calcium Assay Kit (Invitrogen). Cells were loaded with the calcium dye for 30 min at 37 °C in a humidified 5% CO_2 incubator and then at room temperature for a further 30 min. Cells were imaged using a TCS-SP5 confocal microscope (Leica) with a 20x dry objective. Cells were imaged for ~1 min before Bv8 treatment (100nM), and 5-10 min after agonist addition, capturing every 1.2 seconds. Fluorescent intensity values were generated with the Leica LASAF software.

2.10 Computational assembly of the dimers

Modeller 9v8 (Martí-Renom et al., 2000) was used to model TM helices 1-7, and both intracellular and extracellular loops 1-3, of human PKR2 using a combination of both δ-opioid receptor (PDB code 4N6H, Fenalti et al., 2014) and neurotensin receptor 1 structures (PDB code 4GRV, White et al., 2012). Dimers of PKR2 were constructed by aligning the monomers to CXCR4 dimers (PDB code 3ODU, Wu et al., 2010). Modeling figures were generated using PyMOL 1.5.3 (Schrodinger, 2012).

2.11 Statistical analysis

Statistical significance was determined using paired Student's *t*-test. Differences are considered significant at $p<0.05$.

3. Results

3.1 Loss of TMs 5-7 impairs association with WT PKR2 in yeast

In order to identify TM regions that are involved in PKR2 dimerization, progressive deletion mutants were generated at the C-terminal region as detailed in Figure 1. The utility of deletion mutants has been demonstrated by different GPCR studies as receptor fragments can be expressed in a relatively native form (Marsango et al., 2011; Overton and Blumer, 2002; Trettel et al., 2003). Deletion mutants were: TM1-6 with a deletion in the region comprising the seventh TM helix, helix 8 and the C-terminal sequence, TM1-5 lacking the sixth and seventh TM helices, helix 8 and the C-terminal tail and TM1-4 missing the fifth, sixth and seventh TM helices, helix 8 and the C-terminal region. Compared to WT PKR2, whose predicted molecular weight is 44 kDa, the deletion mutants are characterized by reduced size, specifically the predicted molecular weights are: 36 kDa for TM1-6, 27 kDa for TM1-5 and 24 kDa for TM1-4.

Mutant receptors were assessed for their ability to dimerize with either the mutant ΔN term-R2-HIS (43 kDa) (Marsango et al., 2011), untagged mutants or full-length PKR2 by co-immunoprecipitation in yeast. The receptors were immunoprecipitated, subjected to SDS-PAGE, and immunodetected using a commercial polyclonal antibody raised against a peptide corresponding to the amino-terminal 18 amino acids of PKR2, which does not recognize ΔN term-R2-HIS. Interestingly, almost all mutants, when co-expressed together with ΔN term-R2-HIS, retained the ability to co-immunoprecipitate with ΔN term-R2-HIS, as evidenced by the co-immunoprecipitated complexes with molecular weight of ~90 kDa for ΔN term-R2-HIS with WT, ~80 kDa for ΔN term-R2-HIS with TM1-6 and ~72 kDa for those containing ΔN term-R2-HIS with TM1-5 (Fig. 2 A-C right panels). However, ΔN term-R2-HIS did not co-immunoprecipitated with TM1-4, suggesting a role for TM5 in the dimer interface (Fig. 2 D right panel).

3.2 WT-Rluc8 and WT-Venus show functional properties similar to untagged WT PKR2

To understand whether PKR2 could form homo-dimers in live mammalian cells, bioluminescence resonance energy transfer (BRET) was employed. BRET is a biophysical technique used to detect protein-protein interactions that occur within <100Å via a non-radiative transfer of energy from a luminescent donor (*Renilla* luciferase, Rluc) to a fluorescent acceptor (e.g. yellow fluorescent protein, YFP). BRET has been extensively employed to study GPCR-GPCR interactions and conformational changes (Bouvier et al., 2007).

PKR2 was tagged at the intracellular C-terminus with the BRET donor or acceptor molecules, Rluc8 or Venus, which are more stable variants of the classic Rluc and YFP, respectively (De et al., 2007). To ascertain if the C-terminal tagging of the receptor with either Rluc8 or Venus did not alter its function, we compared the activity of the tagged variants to the untagged WT PKR2 in regard to the $G_{\alpha s}$ and $G_{\alpha q}$ pathways. For this purpose a Cre-Luc reporter gene assay and measurement of calcium responses using a fluorescent calcium indicator, Fluo4-AM, were carried out, respectively. CHO cells transfected with WT, WT-Venus or WT-Rluc8 were tested for their ability to activate cAMP-mediated Cre-Luc and increase intracellular calcium levels. Following stimulation with the ligand Bv8 the two BRET-tagged receptors displayed no significant difference in the ability to activate Cre-luciferase or increase intracellular calcium levels compared to untagged WT (Fig. 3 A and B, respectively), indicating that C-terminal tagging of PKR2 did not impact receptor activation.

3.3 Homodimerization of PKR2 in mammalian cells via BRET

HEK 293 cells were co-transfected with WT-Rluc8 and WT-Venus and a BRET saturation curve was generated to demonstrate the ability of PKR2 to form constitutive homodimers under constant donor expression levels and increasing acceptor expression levels (Fig. 4). Saturation of the BRET signal was observed at the higher ratios of energy acceptor to donor and is consistent with a profile predicted for specific interactions between the two receptor protomers (Eidne et al., 2002). The specificity of the interaction was further demonstrated by the ability of untagged WT to inhibit the BRET signal between Rluc8- and Venus-tagged receptors (Fig. 4). Moreover, no inhibition in BRET signal between Rluc8 and Venus-tagged PKR2 was observed when the non-interacting c-FMS (a tyrosine-kinase receptor) was

expressed (Fig. 4). Overall, these results suggest that using BRET, PKR2 is able to form constitutive homodimers in live mammalians cells.

3.4 Specific TM domains determine conformational arrangements of the PKR2 homodimer

To confirm our observations in yeast and further dissect the potential dimer interfaces, truncated forms of PKR2 lacking one or more TMs, as described above, were employed (Fig. 1). We first tested the ability of the full-length WT receptor to form dimers with its truncated forms via BRET. HEK 293 cells were transfected with a constant amount of WT-Rluc8, TM1-6-Rluc8 or TM1-4-Rluc8 with increasing amounts of either WT-Venus or TM1-5-Venus. BRET saturation curves were obtained when WT PKR2 was co-expressed with either TM1-6 or TM1-5 (Fig. 5 B-C). However, BRET signals were not observed when TM1-4-Rluc8 was co-expressed with WT-Venus (Fig. 5 D). These results are consistent with the co-immunoprecipitation data in yeast (Fig. 2).

BRETmax values obtained from saturation curves, which represents the distance between the donor and acceptor tags (Mercier et al., 2002), were significantly lower between WT and TM1-6 compared to WT/WT (Fig. 5 E), suggesting an increase in the distance between donor and acceptor pairs upon loss of TM7 from one protomer of the dimer. In contrast, co-expression of WT-Rluc8 with TM1-5-Venus resulted in a five-fold increase in BRETmax values, indicating a significant decrease in the distance between Rluc8 and Venus molecules upon loss of TM6-7 in one protomer of the dimer. The affinity between the donor and acceptor-tagged proteins is represented by the BRET50, which is the ratio of YFP/Rluc necessary to achieve 50% of the maximal BRET signal (Mercier et al., 2002). Removal of TM7 (TM1-6) or TMs 6 and 7 (TM1-5) in one protomer of the PKR2 dimer resulted in a small decrease in the BRET50 value and a left shift of the curve compared to WT/WT associations, indicating an increase in the affinity of the interaction, however, this was only significant ($p<0.05$) between WT and TM1-6 (Fig. 5 F).

Since the deletion of TMs 6 and 7 in one of the PKR2 protomers dramatically increased the proximity of this truncation mutant to WT PKR2, we then measured the ability of TM1-5 to associate with receptors lacking

either TM7 (TM1-6) or TMs 5-7 (TM1-4) in HEK 293 cells co-transfected with a constant amount of either, TM1-6-Rluc8 or TM1-4-Rluc8 with increasing amounts of TM1-5-Venus. BRET signals between TM1-6 and TM1-5 reached saturation (Fig. 6 B) with a BRETmax value that was not significantly different to signals obtained between WT and TM1-5 (Fig. 6 A-C and 6 D). Unexpectedly, in cells expressing TM1-4-Rluc8 and TM1-5-Venus a saturated BRET profile was observed that was not apparent in cells expressing TM1-4 with WT (Fig. 6 C). However, the BRETmax value was significantly lower than that obtained in cells co-expressing WT with TM1-5 (Fig. 6 D). No significant effect in BRET50 values was observed between any of the TM1-5 combinations (Fig.6 E). These results indicate that TM1-4 can associate with another PKR2 protomer that does not contain TMs 6 and 7, suggesting a possible role of these latter TMs in regulation of the protomer organization within a dimer.

The ability of TM1-4 to interact with TM1-5 but not with WT could be due to either; i) an alternate organization of the protomers in the dimer complex that favors an interaction, not observed between WT and TM1-4, or ii) an impact of TM1-5 on the folding of TM1-4. To distinguish between these possibilities we co-expressed WT-Rluc8 and WT-Venus with or without untagged TM1-4. Expression of TM1-4 inhibited the WT/WT BRET signal, where the linear BRET signals obtained in the presence of TM1-4 indicate a non-specific interaction (Suppl. Fig. 1). This result suggests that TM1-4 can associate with WT, but possibly in a distinct manner from WT/WT interactions. Overall these results suggest a role for TM5 in regulating the spatial distance/orientations of TMs from one of the protomers within the dimer.

3.5 Lack of TMs 6 and 7 positively regulates WT PKR2 signaling and expression

To determine whether altering the association of PKR2 protomers within a dimer has a functional role on PKR2 activity, we measured the signal response of WT PKR2 in the absence or presence of PKR2 lacking either TM 6 and 7 (TM1-5) or TMs 5-7 (TM1-4). For all signaling experiments CHO cells were subsequently employed as HEK 293 cells exhibit endogenous responses to the PKR2 ligand, Bv8, as has been previously reported (Fig. 7 A; Suppl. Fig.2; Lin D.C. et al., 2002). The profile of interactions between PKR2 WT and the truncated receptors via BRET were similar between these two cell types (Suppl. Fig. 3 and Fig. 5 for CHO and HEK 293 cells respectively). CHO cells were transfected with Cre-Luc reporter gene

and either WT, TM1-5, or TM1-4 alone, furthermore WT was co-expressed with either TM1-5 or TM1-4, and Cre-Luc activity was measured. In cells transfected with Cre-Luc only, treatment with Bv8 did not induce a signaling response, (Fig. 7 A). In CHO cells expressing WT PKR2 there was ~3-fold ligand-induced increase over basal in Cre-Luc activity (Fig. 7 A). In contrast, no agonist induced signaling through $G_{\alpha s}$ was observed in CHO cells expressing TM1-4 or TM1-5 alone (Fig. 7 A), consistent with prior observations for the role of residues in intracellular loop 3 and TM6 in G protein signaling of PKR2 (Zhou et al., 2013). Co-expression of WT with TM1-5, but not TM1-4, significantly increased Cre-luc activation (Fig. 7 A). As the increase in signaling of WT PKR2 upon co-expression of TM1-5 could be due to an increase in PKR2 surface expression levels, we measured total surface levels of HA-WT via flow cytometry. Interestingly, normalization of Cre-Luc signaling to surface expression levels of WT indicated that TM1-5, but not TM1-4, significantly increases WT ligand-induced signaling by two fold (Fig. 7 B), as overall WT expression levels were greater when the receptor was expressed alone compared to co-transfectants (mean florescence values for WT expressed alone= 9081.14, mean florescence values for WT in presence of TM1-5= 5203.85). Interestingly, analysis of surface receptor expression via flow cytometry of the cells only co-expressing HA-WT and TM1-5, revealed that expression of TM1-5 increases surface expression of WT by 3-fold compared to cells in the same transfection that only express WT. These data suggests that TM1-5, although a non-functional receptor when expressed alone, can increase surface expression and $G_{\alpha s}$ signaling of WT PKR2.

4. Discussion

Dimerization of GPCRs can modulate specific functional properties of the complex, including ligand binding, signaling, and trafficking (Palczewski, 2010). Therefore, a detailed understanding of the dimer complex assembly provides key mechanistic insight in to how GPCRs regulate a broad array of signaling pathways and systems. We have previously shown that PKR2 forms active dimers in physiologically relevant cell types (Marsango et al., 2011), but knowledge of how organization of protomers within a dimer and which TMs are involved in dimer formation is unknown. In this study we employed two different and

complementary techniques, co-immunoprecipitation and BRET, that provided a mean to dissect the mechanism underlying PKR2 dimerization and to unveil the relative arrangement of the protomers involved (Kaczor and Selent, 2011).

Crystal structures of several GPCRs have presented distinct dimer interfaces, roughly classified into two different types. Type I which involves TM1/H8 was first reported in β_2-adrenergic receptors and more recently in κ-opiod receptor, β_1-adrenergic receptor and in the μ-opioid receptor (Cherezov et al., 2007; Huang et al., 2013; Manglik et al., 2012; Wu et al., 2012). A distinct dimer organization (Type II), which involves mainly TM5 and, parts of TM4 and TM6 was first observed in the crystal structure of the chemokine receptor CXCR4 and subsequently in the μ-opioid receptor and β_1-adrenergic receptor structures (Huang et al., 2013; Manglik et al., 2012; Wu et al., 2010).

The use of truncated forms of PKR2 and the study of their interaction *via* BRET analysis led us to hypothesize dimer arrangement. Although it is not possible to know the relative position of Venus and Rluc8 with respect to the receptor, it seems reasonable to consider that dimers where the interface of interaction is at TM1-2-H8 will have the two fluorescent proteins closer to each other than in the TM4-5-6 complex (Fig. 8 A-B). BRETmax values for WT/WT is low, suggesting that the two fluorescent proteins are relatively far from each other, a situation more probable if the interface involved in dimer formation comprises TM4-5-6. Since the absence of TM6 in the membrane bundle does not statistically affect affinity of the protomers for each other, it is reasonable to conclude TM6 is not directly involved in the dimer interaction interface, thus the WT/WT dimer interface likely involves helices TM4 and TM5 (Fig. 8 C). The interactions between WT/TM1-5 exhibited much closer vicinity between fluorescent proteins than WT/WT, consistent with a TM4-5 dimer interface, as when the fluorescent protein is at the C-terminus of TM5 it places it much closer to the other protomer's C-terminal tag (Fig. 8 D). Therefore, our results confirm a primary role for TM5, indicating that PKR2 likely forms a Type II dimer, in a similar manner to β_1 adrenergic receptor, μ-opioid receptor and CXCR4 (Huang et al., 2013; Manglik et al., 2012; Wu et al., 2010).

TM1-5 also had a positive effect on WT receptor function via an increase in surface expression, suggesting a role of this mutant in promoting the folding of WT PKR2. Furthermore, this mutant could increase agonist-induced $G_{\alpha s}$ signaling, independent of any effect on receptor expression. Given the ability of PKR2 to activate diverse signaling pathways, TM1-5 could positively impact PKR2 activity broadly or specifically to $G_{\alpha s}$ signaling only, as has been reported recently for certain PKR2 missense mutations (Sbai et al., 2014). Studies with several GPCRs show that the co-expression of two mutant receptors, that individually do not bind or transduce signals, results in functional receptors suggesting that receptor-receptor interactions could affect either the ligand-binding pocket, the G protein interface, or possibly even the intermolecular interactions that may directly drive receptor activation (Bouvier, 2001). Although many studies have reported that expression of either natural occurring truncated splice variants, disease-causing mutations or 'designed' truncated receptors can have a dominant negative effect on WT receptor function, primarily due to retention of both receptors in the biosynthetic pathway (Zariñán et al., 2010) there are also non-functional highly-truncated splice variants of GPCRs that can positively regulate WT GPCR activity via stabilization of receptor conformation and increase in receptor expression (Wise, 2012; Xu et al., 2013). However, in this study we also observe a positive impact on WT receptor $G_{\alpha s}$-mediated signaling independent of its effect on WT receptor expression. In the recently solved active-state GPCR structures, TMs 5 and 6 have been shown to undergo significant conformational changes, compared to TMs 1-2. As the Type I dimer principally involves the position and orientation of TM1, upon receptor activation the dimer interface is subject to minimal conformational changes, and as a result, does not impact the other protomer. The Type II dimer, however, is mediated by the TM5 region, very close to where, upon receptor activation, the largest helical rearrangements occur (TM6). Thus, in a Type II dimer, activation of one protomer will affect the dimer interface, which will subsequently alter or signal to the second protomer (Zhu et al., 2013).

Notably, this is the first time that a PKR2 mutant has been shown to have a positive effect on the WT receptor, both on expression and activity. Even though a disease-causing PKR2 'dominant positive' mutant lacking TMs 6-7 has not been described, it is possible that other existing mutants exert similar effects on WT PKR2 activity. Such potential positive effects of mutants on WT PKR2 signaling may help our understanding of KS, where point mutations in both PKR2 and its ligand PK2 have been shown to be responsible for at least 9% of cases, with the majority of patients being heterozygotes for the mutation (Dodé

and Rondard, 2013). KS is a heterogeneous disease, in terms of the variability of the olfactory and reproductive phenotypes and the complexity of its genetic transmission, characterized by incomplete penetrance, suggesting the influence of modifier genes or environmental factors (Sarfati et al., 2010). It has been reported that subjects within a single family heterozygous for the same point mutation in PKR2 exhibit distinct phenotypes, ranging from individuals with absent puberty and anosmia to asymptomatic carriers (Cole et al., 2008). In this context, it is possible that a dominant positive effect of a mutant on the WT receptor may explain why the Kallmann phenotype is not evident in certain individuals. For those members of the family carrying the same mutation in PKR2 yet presenting with the Kallmann phenotype, the manifestation of the disease could be explained by the presence of other mutations in other genes (e.g. KAL1), according to the known oligogenic nature of KS.

In conclusion, this study provides novel information on various structural and functional aspects involved in PKR2 dimerization that may help pave the way to the development of new strategies aimed at interfering with GPCR dimer formation for therapeutic purposes.

References

Ausubel F.M., Brent R., Kingston R., Moore D., Seidman J., Smith J.A .,1994. Editors, current protocols in molecular biology. Wiley, New York.

Bouvier M., 2001. Oligomerization of G-protein-coupled transmitter receptors. Nat. Rev. Neurosci. 2, 274-286.

Bouvier, M., Heveker, N., Jockers, R., Marullo, S., Milligan, G., 2007. BRET analysis of GPCR oligomerization: newer does not mean better. Nat. Methods 4, 3-4.

Chen, J., Kuei, C., Sutton, S., Wilson, S., Yu, J., Kamme, F., Mazur, C., Lovenberg, T., Liu, C., 2005. Identification and pharmacological characterization of prokineticin 2β as a selective ligand for prokineticin receptor 1. Mol. Pharmacol. 67, 2070-2076.

Cheng, M.Y., Bullock, C.M., Li, C., Lee A.G., Bermak, J.C., Belluzzi, J., Weaver, D.R., Leslie F.M., Zhou, Q.Y., 2002. Prokineticin 2 transmits the behavioural circadian rhythm of the suprachiasmatic nucleus. Nature. 417, 405-410.

Cherezov V., Rosenbaum D.M., Hanson M.A., Rasmussen S.G., Thian F.S., Kobilka T.S., Choi H.J., Kuhn P., Weis W.I., Kobilka B.K., Stevens R.C., 2007. High-resolution crystal structure of an engineered human beta2-adrenergic G protein-coupled receptor. Science. 318, 1258-1265.

Cole, L.W., Sidis, Y., Zhang, C., Quinton, R., Plummer, L., Pignatelli, D., Hughes, V.A., Dwyer, A.A., Raivio, T., Hayes, F.J., Seminara, S.B., Huot, C., Alos, N., Speiser, P., Takeshita, A., Van Vliet, G., Pearce, S., Crowley Jr., W.F., Zhou, Q.Y., Pitteloud N., 2008. Mutations in prokineticin 2 and prokineticin receptor 2 genes in human gonadotrophin-releasing hormone deficiency: molecular genetics and clinical spectrum. Clin. Endocrinol. Metab. 93, 3551-3559.

De, A., Loening, A. M., Gambhir, S. S., 2007. An improved bioluminescence resonance energy transfer strategy for imaging intracellular events in single cells and living subjects. Cancer Res. 67, 7175-7183.

Dodé, C., Rondard P., 2013. PROK2/PROKR2 Signaling and Kallmann Syndrome. Front. Endocrinol. 4,19.

Dodé, C., Teixeira, L., Levilliers, J., Fouveaut, C., Bouchard, P., Kottler, M.L., Lespinasse, J., Lienhardt-Roussie, A., Mathieu, M., Moerman, A., Morgan, G., Murat, A., Toublanc, J.E., Wolczynski, S., Delpech, M., Petit, C., Young, J., Hardelin J.P., 2006. Kallmann syndrome: mutations in the genes encoding prokineticin-2 and prokineticin receptor-2. PLoS Genet. 2, e175.

Dowell, S.J., Brown, A.J., 2002. Yeast assays for G-protein-coupled receptors. Receptors Chan. 8, 343-352.

Eidne, K.A., Kroeger, K.M., Hanyaloglu, A.C., 2002. Applications of novel resonance energy transfer techniques to study dynamic hormone receptor interactions in living cells.Trends Endocrinol. Metab. 13, 415-421.

Fenalti, G., Giguere, P. M., Katritch, V., Huang, X.-P., Thompson, A. A., Cherezov, V., Roth, B. L., Stevens, R. C., 2014. Molecular Control of D-Opioid Receptor Signalling. Nature. 1–18.

Giannini, E., Lattanzi, R., Nicotra, A., Campese, A.F., Grazioli, P., Screpanti, I., Balboni, G., Salvadori, S., Sacerdote, P., Negri. L., 2009. The chemokine Bv8/prokineticin 2 is up-regulated in inflammatory granulocytes and modulates inflammatory pain. Proc. Natl. Acad. Sci. U. S. A. 106, 14646-14651.

Huang, J., Chen, S., Zhang, J.J., Huang, X.Y., 2013. Crystal structure of oligomeric β1-adrenergic G protein-coupled receptors in ligand-free basal state. Nat. Struct. Mol. Biol. 20, 419-425.

Kaczor, A.A., Selent, J., 2011. Oligomerization of G protein-coupled receptors: biochemical and biophysical methods. Curr. Med. Chem. 18, 4606-4634.

LeCouter, J., Kowalski, J., Foster, J., Hass, P., Zhang, Z., Dillard-Telm, L., Frantz, G., Rangell, L., DeGuzman, L., Keller, G.A., Peale, F., Gurney, A., Hillan, K.J., Ferrara, N., 2001. Identification of an angiogenic mitogen selective for endocrine gland endothelium. Nature 412, 877-884.

Lin, D.C., Bullock, C.M., Ehlert, F.J., Chen J.L., Tian H., Zhou Q.Y., 2002. Identification and molecular characterization of two closely related G protein-coupled receptors activated by prokineticins/endocrine gland vascular endothelial growth factor. J. Biol. Chem. 277, 19276-19280.

Lin, R., LeCouter, J., Kowalski, J., Ferrara, N., 2002. Characterization of endocrine gland-derived vascular endothelial growth factor signaling in adrenal cortex capillary endothelial cells. J. Biol. Chem. 277, 8724-8729.

Manglik, A., Kruse, A.C., Kobilka, T.S., Thian, F.S., Mathiesen, J.M., Sunahara, R.K., Pardo, L. Weis, W.I, Kobilka, B.K., Granier S., 2012. Crystal structure of the μ-opioid receptor bound to a morphinan antagonist. Nature 485, 321-326.

Marsango, S., Bonaccorsi di Patti, M.C., Barra, D., Miele, R., 2011. Evidence that prokineticin receptor 2 exists as a dimer in vivo. Cell. Mol. Life Sci. 68, 2919-2929.

Martí-Renom, M. A., Stuart, A. C., Fiser, A., Sánchez, R., Melo, F., Sali, A., 2000. Comparative Protein Structure Modeling of Genes and Genomes. Annu. Rev. Biophys Biomol Struct. 29, 291-325.

Mercier, J. F., Salahpour, A., Angers, S., Breit, A., Bouvier, M., 2002. Quantitative assessment of b1- and b2-Adrenergic Receptor Homo- and Heterodimerization by Bioluminescence Resonance Energy Transfer. J. Biol. Chem. 47, 44925-44931.

Miele R., Lattanzi R., Bonaccorsi di Patti M.C., Paiardini A., Negri L., Barra D., 2010. Expression of Bv8 in Pichia pastoris to identify structural features for receptor binding. Protein Expr. Purif. 73, 10-14.

Ng, K.L., Li, J.D., Cheng, M.Y., Leslie, F.M., Lee, A.G., Zhou, Q.Y., 2005. Dependence of olfactory bulb neurogenesis on prokineticin 2 signaling. Science 308, 1923-1927.

Ngan, E.S., Tam, P.K., 2008. Prokineticin-signaling pathway. Int. J. Biochem. Cell. Biol. 40, 1679-1684.

Overton M.C, Blumer K.J., 2002. The extracellular N-terminal domain and TM domains 1 and 2 mediate oligomerization of a yeast G protein-coupled receptor . J Biol Chem. 277, 41463-41472.

Palczewski K., 2010. Oligomeric forms of G protein-coupled receptors (GPCRs). Trends Biochem. Sci. 35, 595-600.

Pitteloud, N., Zhang, C., Pignatelli, D., Li, J.D., Raivio, T., Cole, L.W., Plummer, L., Jacobson-Dickman, E.E, Mellon, P.L., Zhou, Q.Y., Crowley Jr., W.F., 2007. Loss-of-function mutation in the prokineticin 2 gene causes Kallmann syndrome and normosmic idiopathic hypogonadotropic hypogonadism. Proc. Natl. Acad. Sci. U. S. A. 104, 17447-17452.

Rivero-Müller, A., Jonas, K.C., Hanyaloglu, A.C., Huhtaniemi, I., 2013. Di/oligomerization of GPCRs-mechanisms and functional significance. Prog. Mol. Biol. Transl. Sci. 117, 163-185.

Sarfati, J., Guiochon-Mantel, A., Rondard, P., Arnulf, I., Garcia-Piñero, A., Wolczynski, S., Brailly-Tabard, S., Bidet, M., Ramos-Arroyo, M., Mathieu, M., Lienhardt-Roussie, A., Morgan, G., Turki, Z., Bremont, C., Lespinasse, J., Du Boullay, H., Chabbert-Buffet, N., Jacquemont, S., Reach, G., De Talence, N., Tonella, P., Conrad, B., Despert, F., Delobel, B., Brue, T., Bouvattier, C., Cabrol, S., Pugeat, M., Murat, A., Bouchard, P., Hardelin, J.P., Dodé, C., Young, J., 2010. A comparative phenotypic study of kallmann syndrome patients carrying monoallelic and biallelic mutations in the prokineticin 2 or prokineticin receptor 2 genes. J. Clin. Endocrinol. Metab. 95, 659-69.

Sbai, O., Monnier, C., Dodé, C., Pin, J.P., Hardelin, J.P., Rondard, P., 2014. Biased signaling through G-protein-coupled PROKR2 receptors harboring missense mutations. FASEB J. 28, 3734-44.

Schrodinger L., 2012. The PyMOL Molecular Graphics System, Version 1.5r3.

Shojaei, F., Wu, X., Zhong, C., Yu, L., Liang, X.H., Yao, J., Blanchard, D., Bais, C., Peale, F.V., van Bruggen, N., Ho, C., Ross, J., Tan, M., Carano, R.A., Meng, Y.G., Ferrara N., 2007. Bv8 regulates myeloid-cell-dependent tumour angiogenesis. Nature 450, 825-831.

Trettel, F., Di Bartolomeo, S., Lauro, C., Catalano, M., Ciotti, M.T., Limatola, C., 2003. Ligand-independent CXCR2 dimerization. J Biol. Chem. 278, 40980-40988.

White J.F., Noinaj N., Shibata Y., Love J., Kloss B., Xu F., Gvozdenovic-Jeremic J., Shah P., Shiloach J., Tate C.G., Grisshammer R., 2012. Structure of the agonist-bound neurotensin receptor. Nature. 490, 508-513.

Wise H., 2012. The roles played by highly truncated splice variants of G protein-coupled receptors. J. Mol. Signal. 7, 1-13.

Wu, B., Chien, E.Y., Mol, C.D., Fenalti, G., Liu, W., Katritch, V., Abagyan, R., Brooun, A., Wells, P., Bi, F.C., Hamel, D.J., Kuhn, P., Handel, T.M., Cherezov, V., Stevens, R.C., 2010. Structures of the CXCR4 chemokine GPCR with small-molecule and cyclic peptide antagonists. Science, 330, 1066-1071.

Wu, H., Wacker, D., Mileni, M., Katritch, V., Han, G.W., Vardy, E., Liu, W., Thompson, A.A., Huang, X.P., Carroll, F.I., Mascarella, S.W., Westkaemper, R.B., Mosier, P.D., Roth, B.L., Cherezov V., Stevens R.C., 2012. Structure of the human κ-opioid receptor in complex with JDTic. 485, 327-332.

Xu J., Xu M., Brown T., Rossi G.C., Hurd Y.L., Inturrisi C.E., Pasternak G.W., Pan Y.X., 2013. Stabilization of the μ-opioid receptor by truncated single transmembrane splice variants through a chaperone-like action. J. Biol. Chem. 28, 21211-21227.

Zariñán, T., Perez-Solís, M.A., Maya-Núñez, G., Casas-González, P., Conn, P.M., Dias, J.A., Ulloa-Aguirre A., 2010. Dominant negative effects of human follicle-stimulating hormone receptor expression-deficient mutants on wild-type receptor cell surface expression. Rescue of oligomerization-dependent defective receptor expression by using cognate decoys. Mol. Cell. Endocrinol. 321, 112-122.

Zhou, X.T., Chen, D.N., Xie, Z.Q., Peng, Z., Xia, K.D., Liu, H.D., Liu, W., Su, B., Li, J.D., 2013. Functional analysis of the distal region of the third intracellular loop of PROKR2. Biochem. Biophys. Res. Commun. 439, 12-17.

Zhu, L., Zhao, Q., Wu, B., 2013. Structure-based studies of chemokine receptors. Current Opinion in Struct. Biol. 23, 539-546.

FIG 1. Schematic representation of WT and truncated PKR2 constructs used in this study. WT PKR2 constructs used in this study are untagged WT, HA-WT, WT-Rluc8, WT-Venus (left panel). Truncated PKR2 mutants used in this study are ΔNter-PKR2-HIS, PKR2, TM1-6, TM1-6-Rluc8, TM1-5, TM1-5-Venus, TM1-4, TM1-4-Rluc8 (right panel).

FIG 2. Identification of PKR2 TM domains involved in PKR2 dimerization in yeast via co-immunoprecipitation. Membranes from yeast co-expressing ΔN-ter-PKR2-HIS and either WT, TM1-6, TM1-5 or TM1-4 were immunoprecipitated using a Ni-NTA His•Bind Resin and the immunoprecipitates resolved by SDS-page. The immunoblots were probed with anti-HIS (left panels) and anti-PKR2 (right panels) antibodies. Lane 1, ΔNter-PKR2-HIS/WT PKR2 or TM1-6 or TM1-5 or TM1-4; lane 2, Cy; lane 3, ΔNter-PKR2-HIS.

FIG 3. C-terminal tagging of PKR2 with Rluc8 or Venus does not significantly affect receptor function. CHO cells transfected with untagged WT, WT-Venus or WT-Rluc8 were stimulated with Bv8 (100 nM) and tested for their ability to activate Cre-Luc (A) or calcium release (B) (see Materials and Methods). Data is presented as a fold change over untreated (basal) and is the mean $\pm$ SEM of n=4 (A); data is presented as maximal fluorescent intensities and is mean $\pm$ SEM of n=3 (B).

FIG 4. PKR2 forms constitutive dimers in mammalian cells via BRET. HEK 293 cells were transfected with WT tagged with either Rluc8 or Venus. WT-Rluc8 was transfected at a constant amount with increasing amounts of WT-Venus. To further determine specificity in BRET signals cells were also co-transfected with either untagged WT PKR2 or cFMS. BRET measurements were obtained as described in Materials and Methods. Shown is a representative BRET saturation curve of n=5.

FIG 5. Identification of TM domains that regulate PKR2 protomer proximity and affinity. A-D) HEK 293 cells were transfected with a constant amount of either WT-Rluc8, TM1-6-Rluc8 or TM1-4-Rluc8 with increasing concentrations of either WT-Venus or TM1-5-Venus and BRET measurements taken. Plots shown are representative BRET saturation curves of n=5. E) Average maximal net BRET values (BRETmax) indicate distance between Rluc8- and Venus-tagged receptors (n=5). **p<0.01, *p<0.05. F) Average BRET50 values taken from the Venus/Rluc8 ratio that gives 50% of the maximal net BRET signal, and representing the affinity of associations between the two proteins. *p<0.05.

FIG 6. TM5 may positively regulate PKR2 protomer proximity. HEK 293 cells were transfected with constant amounts of either: A) WT-Rluc8, B) TM1-6-Rluc8 or C) TM1-4-Rluc8 and increasing amounts of TM1-5-Venus. D) Average maximal net BRET values (BRETmax) from A-C (n=5). **p<0.01, *p<0.05. E) Average BRET50 values representing the Venus/Rluc8 ratio that gives 50% of the maximal net BRET signal. *p<0.05.

FIG 7. TM1-5 positively regulates WT receptor signaling and expression. A) CHO cells were transfected with HA-WT, TM1-5-Venus or TM1-4. The latter two truncated mutants were also co-expressed with HA-WT. All cells were co-expressed with Cre-Luc and Rluc as a normalization control. Cells were treated with ligand Bv8 (100 nM) for 5 h and assayed for Cre-Luc activity. Values were normalised to Rluc activity and results are expressed as fold change over basal. Mean $\pm$ SEM n=4. *p<0.05, **p<0.01. B) The same cells assayed in (A) that were expressing HA-WT, with and without TM1-5-Venus or TM1-4, were also used to quantitate surface levels of HA-PKR2 via flow cytometry. Cells were treated with anti-HA antibody followed by Alexa Fluor 647 conjugated secondary antibody. The mean fluorescence values were used to

normalize the Cre-Luc data in (A) and expressed as Mean ± SEM of n=4. ***p<0.001. C) Surface expression levels of HA-WT in cells only co-expressing HA-WT and TM1-5-Venus, compared to cells only expressing HA-WT within the same sample, from the same transfectants used in (A-B) were quantified via flow cytometry. The mean fluorescence values of HA-WT are expressed as Mean ± SEM of n=4.

FIG 8. Spatial arrangement of TM domains involved in the dimerization interface of PKR2 dimers. A) Schematic representation of known dimers organized with a Type I dimer, which involves TM1, TM2 and H8, as observed in crystals of β_1-adrenergic receptor, β_2-adrenergic receptor, κ-opioid receptor and μ-opioid receptor, and of B) Type II dimer, with the pivotal role of TM5, and parts of TM4 or TM6 as observed in β_1-adrenergic receptor, CXCR4 and μ-opioid receptor (represented in the scheme). C) Model dimer of WT/WT PKR2. D) Model dimer of WT/TM1-5 PKR2 (red: TM5, light blue: TM6). Relative position of Rluc8 (green cartoon) and Venus (yellow cartoon) are arbitrary but are placed according to experimental results (see Discussion).

Highlights

- Prokineticin receptor 2 (PKR2) forms constitutive dimers in yeast and mammalian cells
- Loss of TM 6 and 7 modulates PKR2 protomer proximity and affinity
- A truncated PKR2 (TM1-5) positively regulates WT receptor expression and signaling
- PKR2 dimer interface likely forms a Type II dimer via TMs 4 and 5

Table

Table 1. Oligonucleotides used for construction of the various mutants

Oligonucleotide	Sequence
R2 BamHI up	5'-ATA GGA TCC ATG GCA GCC CAG AA T GG-3'
R2 HindIII up	5'-ATA AAG CTT ATG GCA GCC CAG AA T GG-3'
TM1 -6 dw	5'-CTC GAG CGG CCG CCA CGT GCT GGA TAT CTG CAG-3'
TM1 -5 dw	5'-GTC GAC ACG AA C TCG ACA CCA AAG ATG-3'
TM1 -4 dw	5'-TGG TCG ACA GGC CAG ATC TGG CCA CAG AAG ATC-3'
R2 SalI dw	5'-ATG TCG ACC TT C AG C CTG ATA CAG TCC-3'

Figure 1

Figure 1

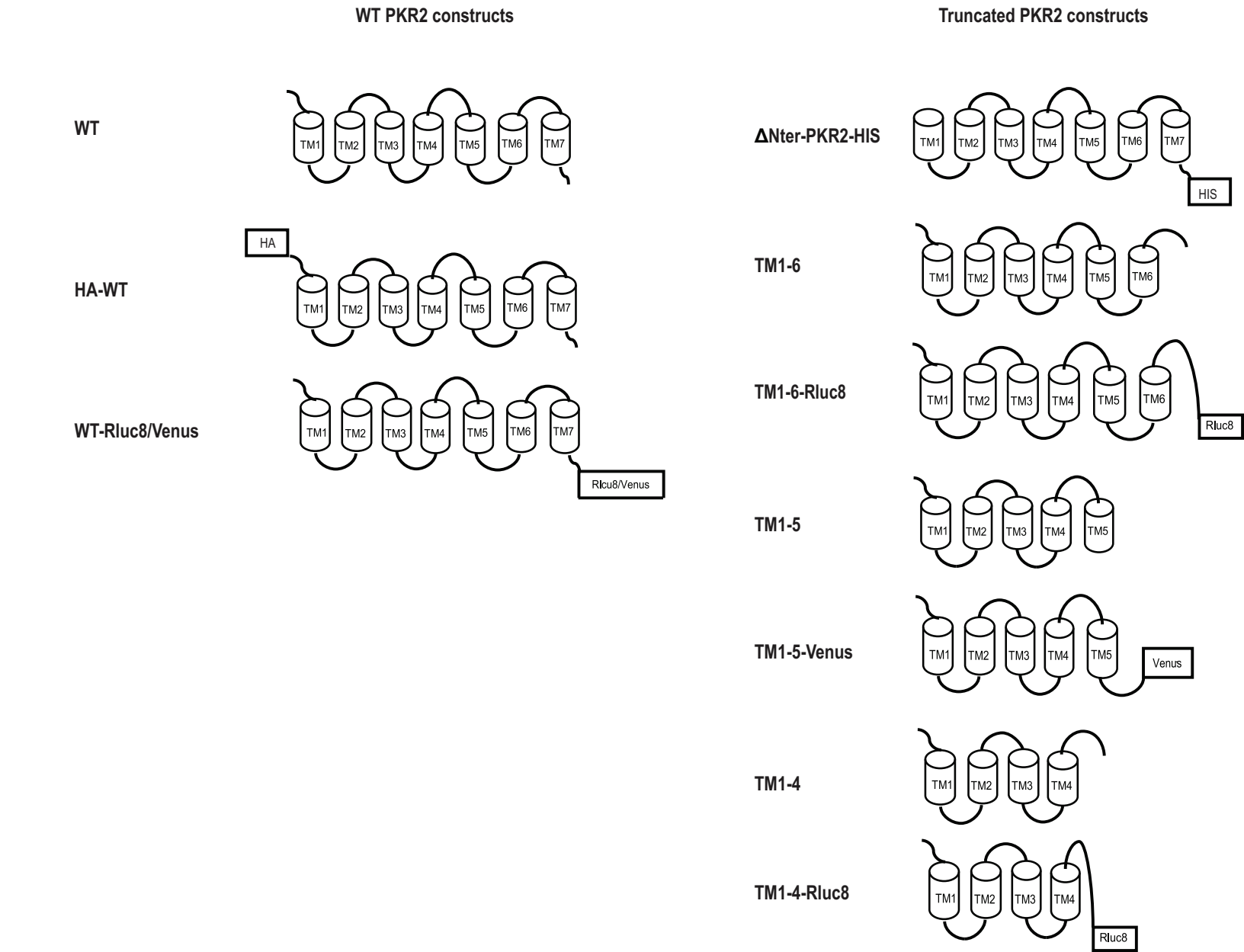

Figure 2

Click here to download high resolution image

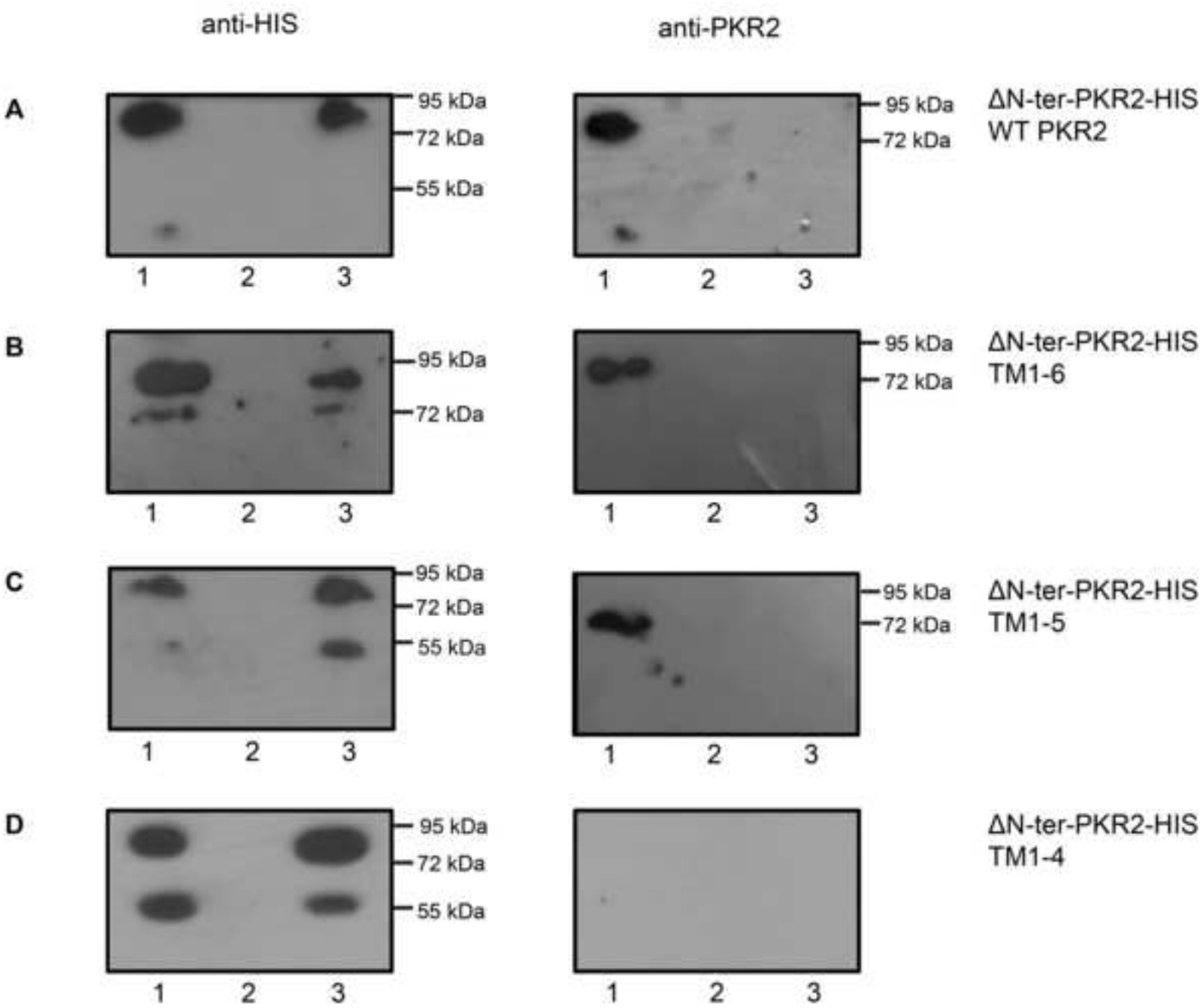

Figure 3

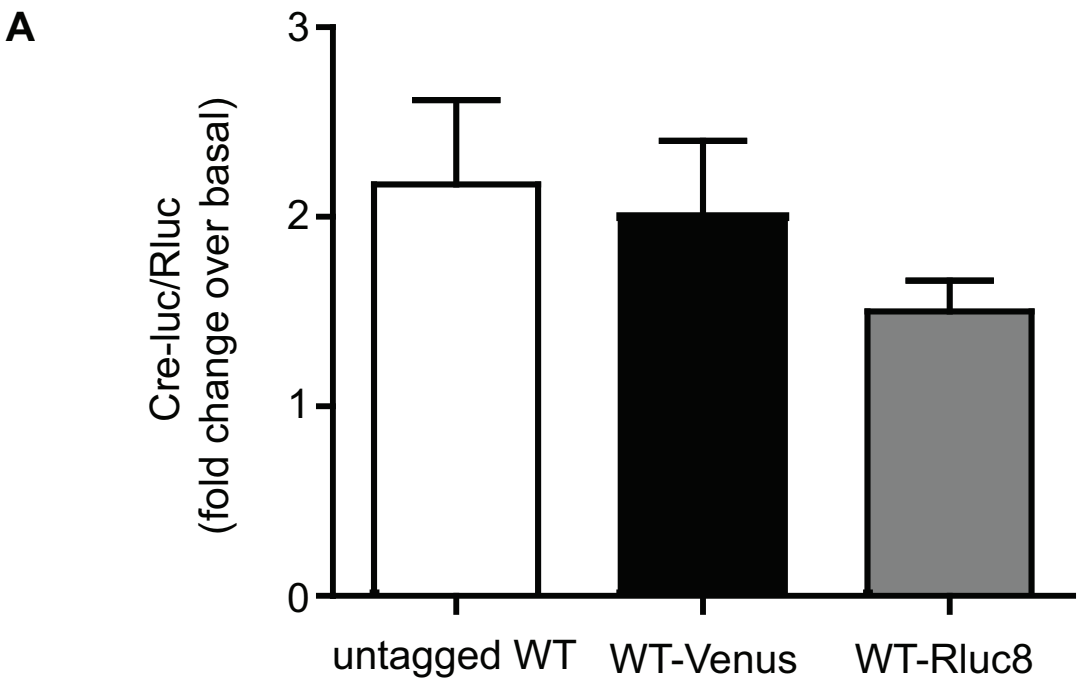
A
Cre-luc/Rluc
(fold change over basal)
3
2
1
0
untagged WT
WT-Venus
WT-Rluc8

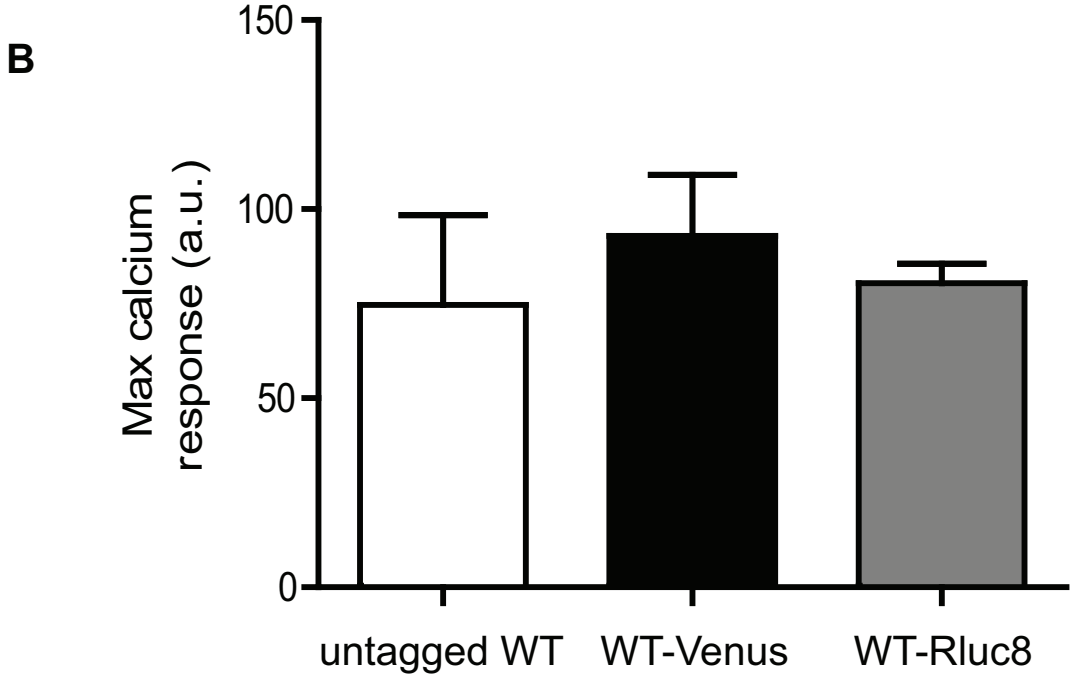
B
Max calcium
response (a.u.)
150
100
50
0
untagged WT
WT-Venus
WT-Rluc8

Figure 4

Figure 4

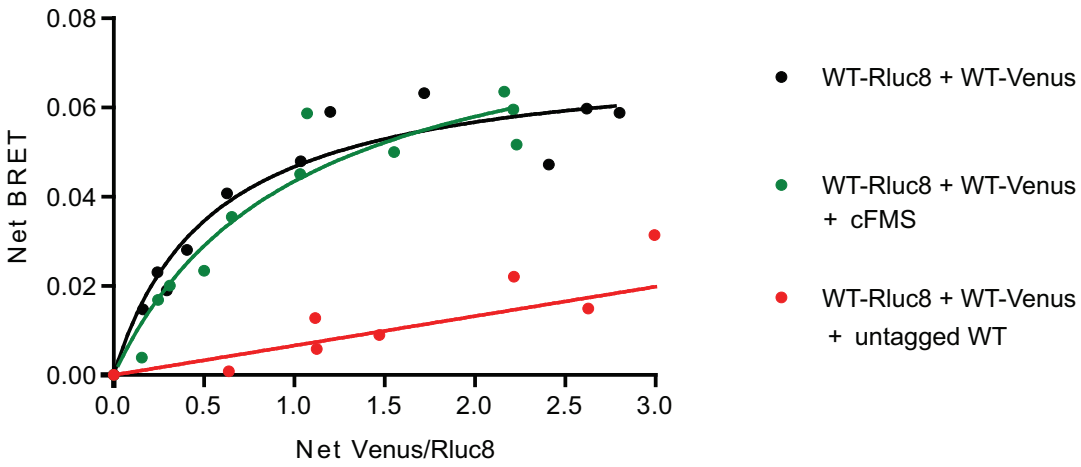

Figure 5

Figure 5

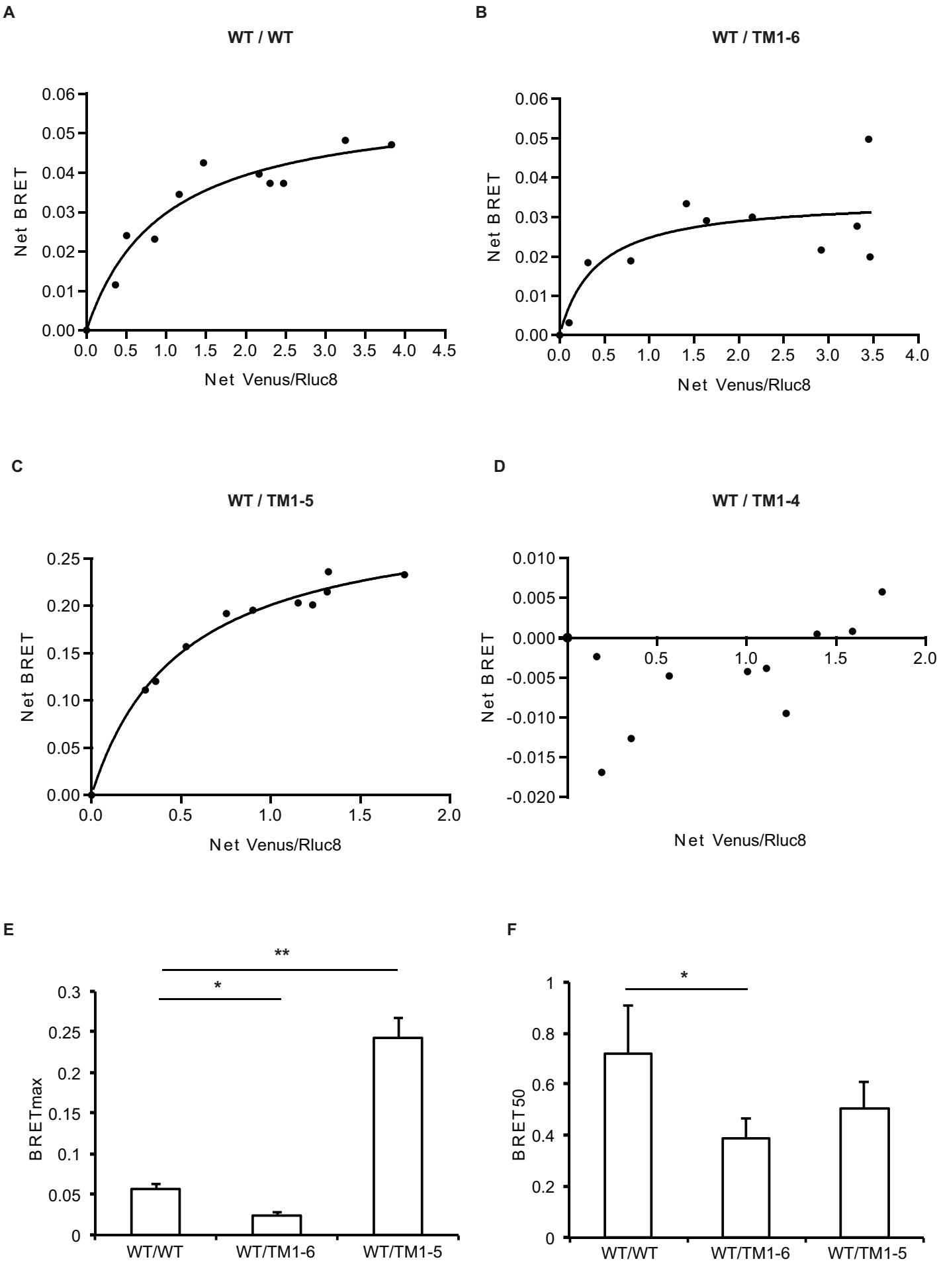

Figure 6

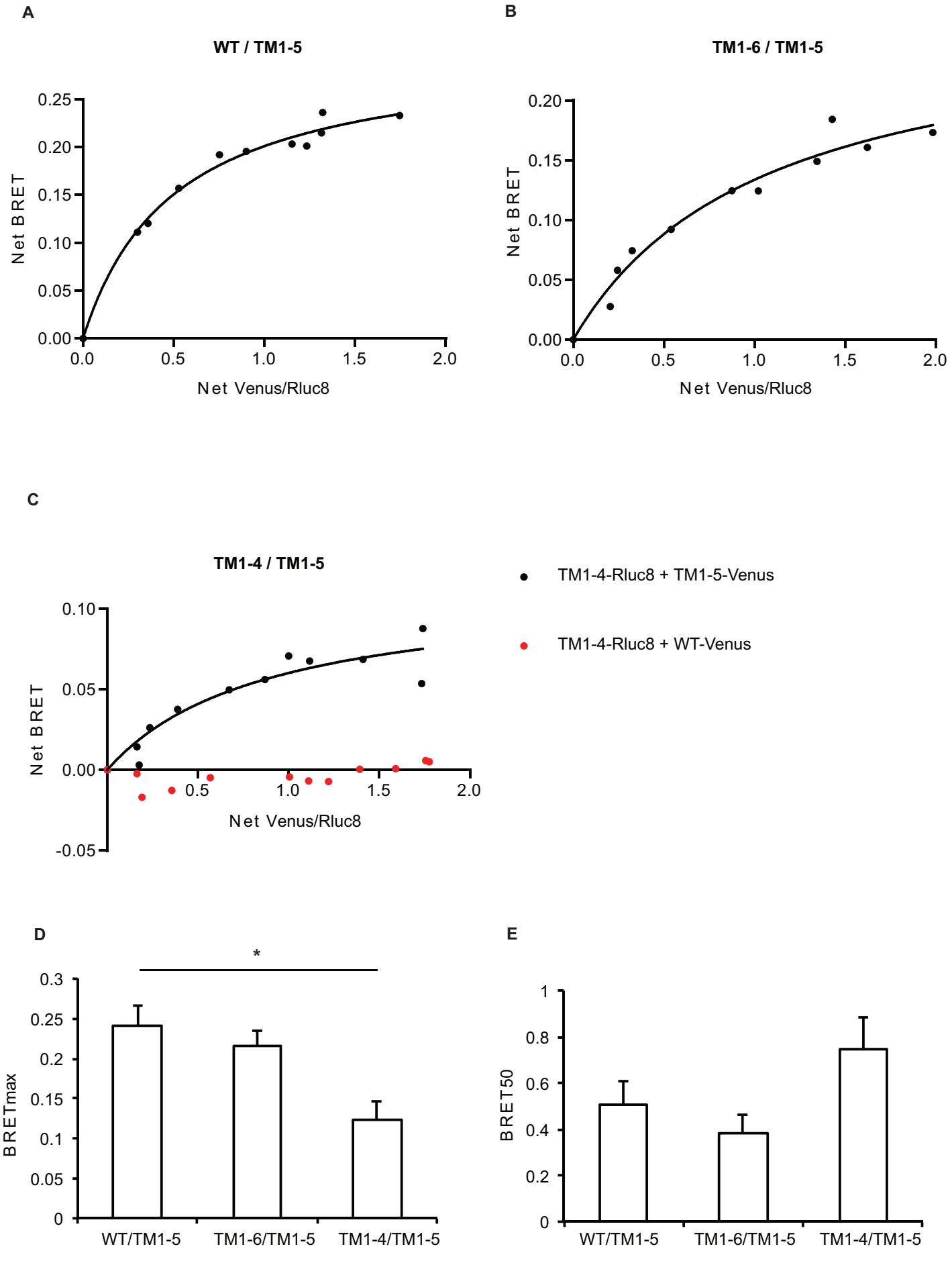
A
WT / TM1-5
Net BRET
Net Venus/Rluc8
B
TM1-6 / TM1-5
Net BRET
Net Venus/Rluc8
C
TM1-4 / TM1-5
Net BRET
Net Venus/Rluc8
TM1-4-Rluc8 + TM1-5-Venus
TM1-4-Rluc8 + WT-Venus
D
BRETmax
*
WT/TM1-5
TM1-6/TM1-5
TM1-4/TM1-5
E
BRET50
WT/TM1-5
TM1-6/TM1-5
TM1-4/TM1-5

Figure 7

Figure 7

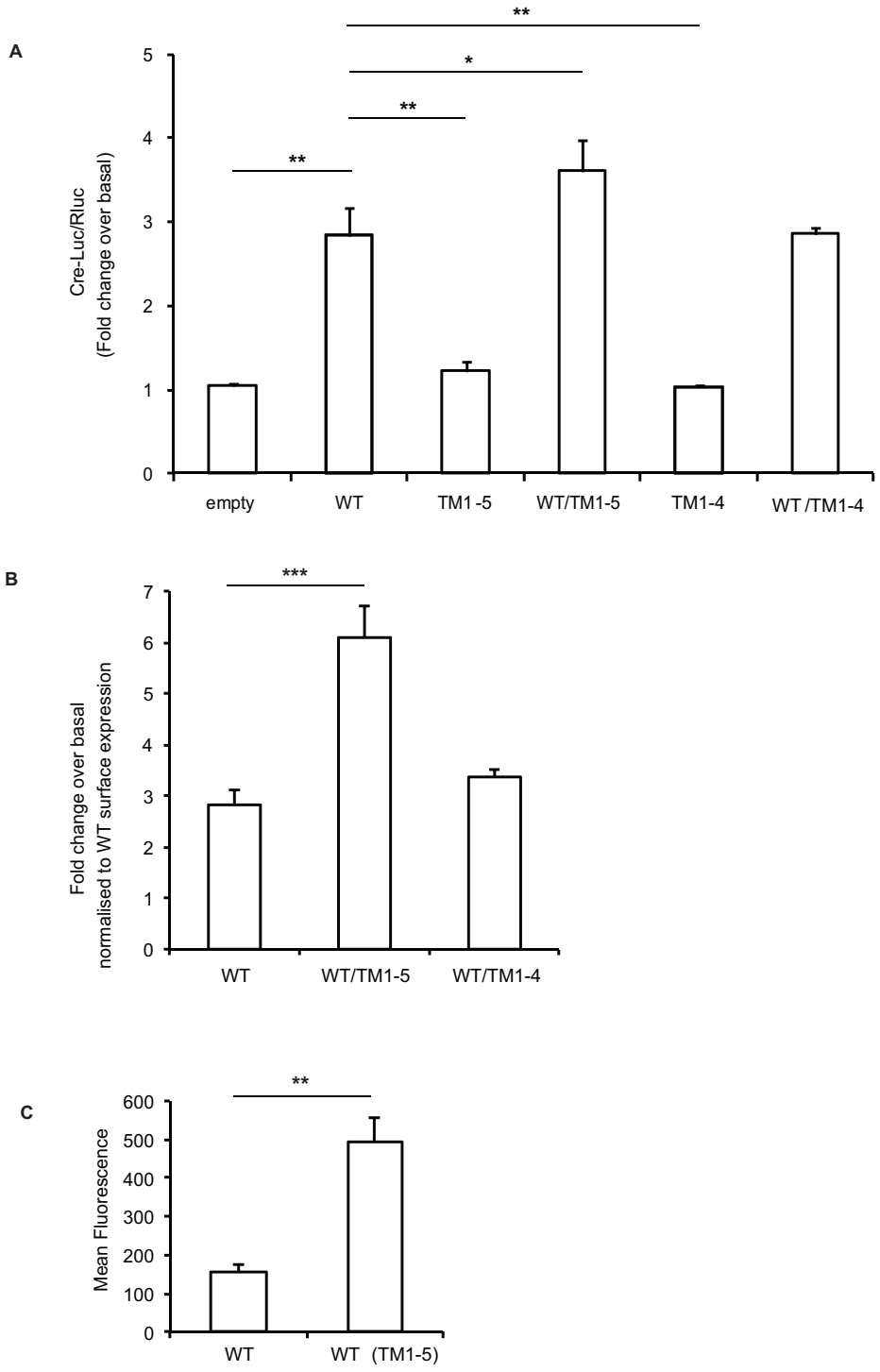

Figure 8
Click here to download high resolution image

Figure 8

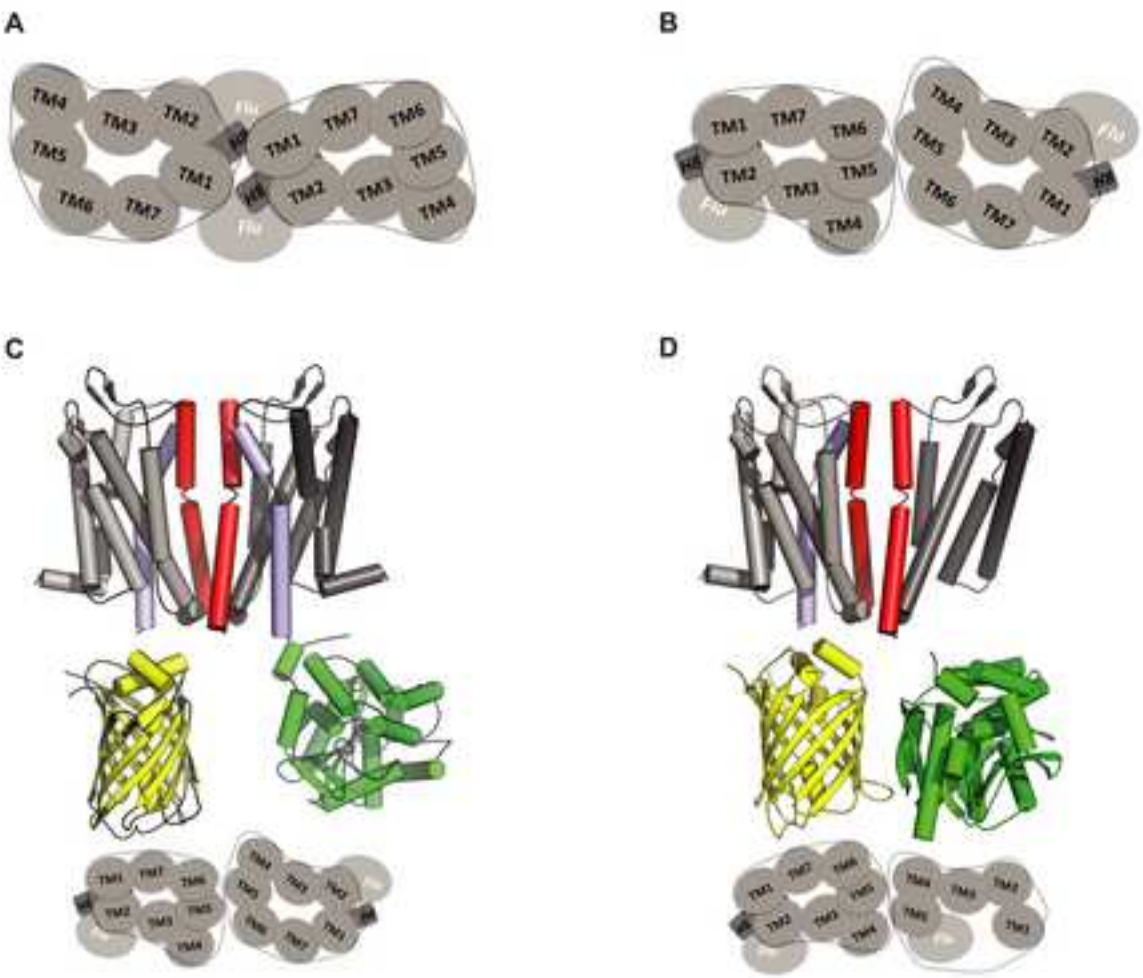

Supplementary Figure 1

Click here to download Supplementary Material: SUPP FIG1.EPS.eps

Supplementary Figure 2

Click here to download Supplementary Material: SUPP FIG2.JPG.JPG

Supplementary Figure 3

Click here to download Supplementary Material: SUPP FIG3.EPS.eps

Supplementary figure legends and methods

Click here to download Supplementary Material: Supplementary Data.docx